ACIDITY OF LANTHANIDE CLUSTER

A Thesis

Presented to

The Graduate Faculty of The University of Akron

In Partial Fulfillment

of the Requirements for the Degree

Master of Science

Xiaohan Xu

April, 2021

ACIDITY OF LANTHANIDE CLUSTERS

Xiaohan Xu

Thesis

Approved:	Accepted:
________________________________ Advisor Dr. Tianbo Liu	________________________________ Interim Director of SPSPE Dr. Ali Dhinojwala
________________________________ Committee Member Dr. Toshikazu Miyoshi	________________________________ Interim Dean of the College Dr. Craig Menzemer
	________________________________ Interim Director, Graduate School Dr. Marnie Saunders
	________________________________ Date

ABSTRACT

Polyoxometalates (POMs) are a large group of metal oxide clusters with well-defined structures, diverse properties, and various applications. Since solutions of metal aquo complexes can protonate their coordinated water ligands, some POMs can behave like weak Brønsted nanoacids. Playing an important role not only in the solution behaviors but also in applications as catalysts and biologically active materials, the acidity of POMs is sometimes related to their deprotonation behaviors. Therefore, studies on the deprotonation of POMs can help people understand the nature of POMs, especially the acidity feature, to further explore POM-based materials and devices.

In this work, a series of lanthanide clusters are applied as model systems to understand the deprotonation of the clusters, which is related to the relative strength of coordinated water molecules and determines the acidity feature of the POM cluster. With potassium ions as counterions, these lanthanide clusters are macroanions in aqueous solutions. The aqueous solutions of the POMs have certain pH values and conductivity, and there is no proton released or absorbed. But the addition of base can trigger deprotonation from the lanthanide clusters. It was found that these lanthanide clusters demonstrated different deprotonation capacity, and according different acidity features. This acidity variation might derive from the difference among lanthanide ions caused by lanthanide contraction.

ACKNOWLEDGEMENTS

I would like to express my sincere gratitude to my adviser, Dr. Tianbo Liu, for inspiring my strong interest in this area and providing the opportunity for me to conduct this project. It is his patient guidance and encouragement that inspires me to explore science, overcome obstacles and challenge myself. I also want to address my great appreciation to Yuqing Yang, our senior group member, for her considerate help on the projects and my studies at UA. I also want to thank Dr. Xinyu Sun, Ehsan Raee and Dr. Jiahui Chen for their great help on experiments and studies, and Dr. Dongdi Zhang for providing high-quality samples for the project. Besides, I would like to thank Dr. Toshikazu Miyoshi for being my committee member and encouraging me and giving helpful suggestions at every stage of my studies. Finally, I appreciate all our group members for their help and inspiration, and my family and friends.

TABLE OF CONTENTS

LIST OF TABLES

LIST OF FIGURES

LIST OF SCHEMES

CHAPTER I

INTRODUCTION

1.1. Introduction of polyoxometalate macroions

1.1.1. Overview of macroions

Electrolyte solutions are complex systems and poorly understood due to the coexistence of intermolecular and intramolecular interactions.[1] Based on electrolyte sizes, electrolyte solutions can be classified into solutions of simple ions (< 1nm) and colloid suspensions (10 nm ~ 100 nm), which are well understood by Debye-Hückel theory and Derjaguin-Landau-Verwey-Overbeek theory (DLVO theory) respectively.[2–4] Whereas, there is a theory gap between simple ions and colloids, inspiring studies on macroions with sizes ranging between 1 and 10 nm. These large ions cannot be considered either as point charges like simple small ions because they cannot be treated as point charges, or colloidal suspensions because they form homogeneous "real solutions". In general, these macroions are highly charged ions with well-defined molecular structure and unique solution behaviors, which is different from simple ions and colloids, therefore providing ideal model systems to understand polyelectrolyte solutions. Typical macroions include bio-macromolecules[5], polyoxometalates (POMs)[1], dendrimers[6], and metal−organic cages (MOC)[7], etc.

1.1.2. Introduction to polyoxometalates

Polyoxometalates (POMs), a class of inorganic compounds with electronic versatility and structural variation, has attracted extensive attention in recent years and has been widely explored in chemistry, physics, materials science, catalysis, medicine, and biology.[8] POMs are a family of metal-oxide anion clusters composed of early transition metals (usually Mo, W, V, Nb, and Ta) with high oxidation states. The giant anion clusters are made up of transition metal oxide polyhedrons, which are linked by sharing oxygen atoms between metal and/or hetero ions. [9]

In 1826, the first POM structure, ammonium phosphomolybdate consisting of $PMo_{12}O^{3-}{}_{40}$ anion, was discovered.[10] Keggin structure was reported after that in 1934 by Keggin, possessing formula $[XO_4M_{12}O_{36}]_n$.[11] Typical types of POMs include Keggin, Lindqvist, Dawson, and Anderson, etc., and a variety of POMs have been explored on their synthesis, characterization, and wide applications. Figure 1.1 shows some examples of POMs with different topologies and sizes. Based on composition and structure, POMs can be classified into two categories: POMs of the general formula $[M_mO_y]^{n-}$ containing only one transition metal and oxygen are named iso-polyoxometalates; compounds including a small number of additional elements $[X_xM_mO_y]^{n-}$ (X = heteroelement, x smaller than m) are considered as hetero-polyoxometalates.[12] Based on charge natures, POMs can be classified into two categories: strong electrolytes, in which group POMs carry inherent charges in crystals balanced by multiple small cations, while usually carry negative charges in solution; and weak electrolytes, in which group POMs are almost neutral clusters in crystals, but their coordinated water ligands attached to non-Mo (or non-W) metals can partially deprotonate in aqueous solution, leading to their weak nano-acid features.[1]

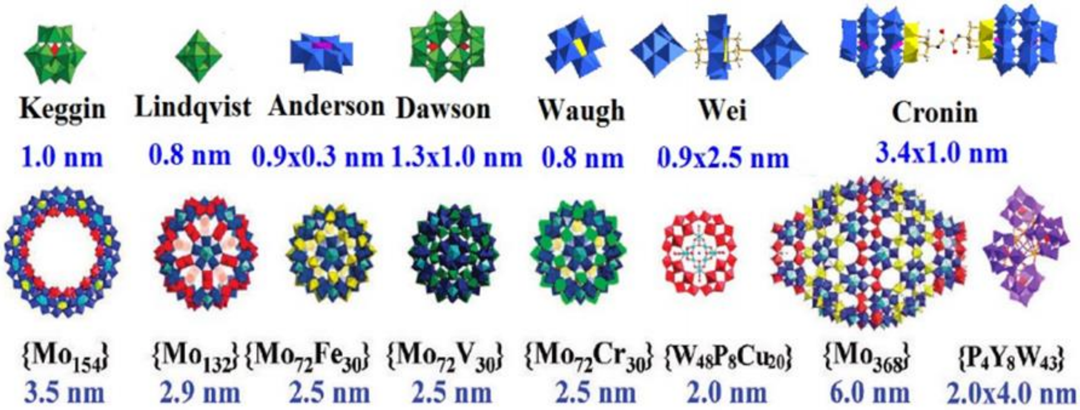

Figure 1.1. POM macroions with different topologies and sizes. Copyright ©2011 Wiley-VCH

POMs demonstrate extreme variability in molecular composition, size, shape, charge density, redox potentials, acidity, and solubility. The diversity of POMs mainly stems from the fact that most elements can be incorporated into the structural framework of POMs, and increasing synthetic reactions have been developed to replace one or more metal centers, organic functions, or organometallic constituent parent POM structures.[13] Under the significant impact of surrounding counterion/co-ion, as well as other approaches, the solution behavior of POMs can be regulated, which enables great solubility and unusual behaviors in nearly all media from water to hydrocarbons. Owing to the excess of oxo ligands over metal ions, POMs usually exist as macroanions in solution.

1.2. Deprotonation of POMs

1.2.1. Overview of solution behaviors of POMs

As large, hydrophilic anions in water and other polar solvents, POMs demonstrate unique solution behaviors by self-assembling into single-layer, hollow, spherical “blackberry” structures, which is quite different from small simple ions and large colloids.[14] The major driving force has been proved to be the counterion-mediated interaction.[15]

Based on the self-assembly of POMs, some intriguing solution behaviors were studied, including the behaviors of the counterions around POM clusters, the control of assembly-disassembly and blackberry size, permeability of the blackberry “membrane” to small cations, the self-recognition behaviors during self-assembly, etc.[16] For certain POMs, some of these solution behaviors are closely related to the deprotonation of POMs, which are briefly introduced hereinbelow.

The tunable self-assembly and blackberry size of POMs such as $\{Mo_{72}Fe_{30}\}$ is attributed to the variation of deprotonations and of the corresponding (average) net charges on the clusters caused by changes of the pH.[17] $\{Mo_{72}Fe_{30}\}$ clusters exert increasing deprotonation capacity with increasing pH, leading to higher surface charges, and accordingly smaller blackberries. (Figure 1.2) Besides, POMs can self-recognize each other in a mixed solution and assemble into two types of homogeneous blackberries, which sometimes also involves the contribution of deprotonation of POM clusters. [18]

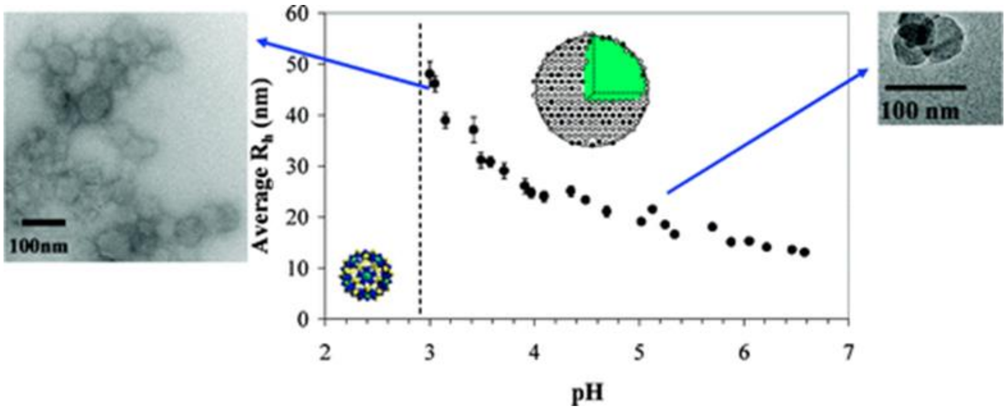

Figure 1.2. Average hydrodynamic radii (R_h) of the blackberries formed in 0.5 mg/mL aqueous solutions of $\{Mo_{72}Fe_{30}\}$ at different pH, measured by DLS. TEM images of the aggregates on carbon film are formed at pH ≈ 3.0 (left; conventional TEM) and pH ≈ 4.6 (right; more appropriate cryo-TEM). Copyright © 2006 American Chemical Society.

1.2.2. Deprotonation from aquo ligands

Since the solutions of metal aquo complexes can protonate their water ligands,[19] some POMs are reported to show deprotonation and behave like weak Brønsted nanoacids.[20–27]

A typical example of POMs with this interesting feature is the $\{Mo_{72}Fe_{30}\}$ cluster, a Keplerate-type POM, as well as its derivatives[18], which can be considered as a nanoacid due to the existence of 30 $Fe^{III}(H_2O)$ groups on the surface that allow pH-dependent deprotonations.[23] For these clusters, the deprotonation process can be initiated once they are dissolved in water, and this behavior is very well-described for the classical

$[Fe^{III}(H_2O)_6]^{3+}$ (Scheme 1).[28] It was proved that each $\{Mo_{72}Fe_{30}\}$ cluster released about 4 protons and 22 protons at pH=3.2 and pH=4.9, respectively, suggesting a pronounced increase of the charge on the clusters with increasing pH.[23] This change of surface charges exerts a great influence on other solution behaviors of the POM clusters, such as tunable self-assembly behaviors discussed in section 1.2.1. Besides, the deprotonation process becomes less favorable as the accumulation of negative surface charges.

$$\cdots Fe^{III}(OH_2)^{3+} + H_2O \Leftrightarrow \cdots Fe^{III}(OH)^{2+} + H_3O^+$$

Schema 1.1. Deprotonation/protonation equilibrium of a water ligand coordinated to a Fe^{III} within large clusters.

Recently, a reversible deprotonation/protonation process of the coordinated water ligands from POM clusters was reported. (Figure 1.3)[27] The POM cluster with the formula $K_{41}[(P_2W_{12}Nb_6O_{62})_6\{Mn_3(OH)_3(H_2O)_6\}_4\{Mn_3Na(H_2O)_{16}\}]\cdot 26H_2O$ is a weak acid in aqueous solution but can release up to 40 protons upon the addition of base, after which the cluster can also absorb about 11 protons with the addition of acid. At the same time, this cluster shows high stability when large amounts of the base are introduced to the solution, which differs from other POMs and enables the possibility of expanded application.

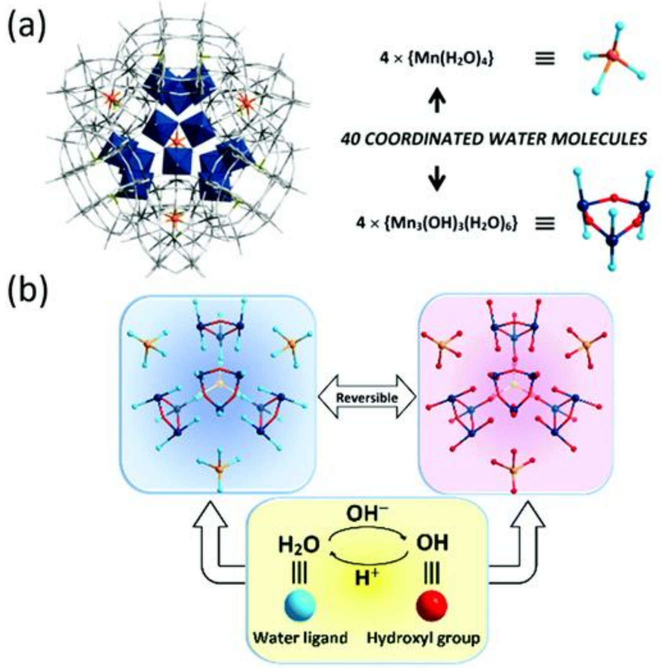

Figure 1.3. a). Representation of POM structure through polyhedral/ball-and-stick. Color code: MnO_6 octahedra (dark teal), Mn/Na spheres (light orange), W/Nb/O (gray), and P (dark yellow). b). Illustration of the reversible protonation and deprotonation process upon base/acid titration. Water ligand is used as an example here. Copyright © The Royal Society of Chemistry 2020

1.2.3. Deprotonation from lacunary cavities

Some POMs without coordinated aquo ligands are also capable of deprotonation. For example, four acidic protons on the lacunary sites of a Keggin-type POM can be neutralized by TBAOH in DMSO.[24,29] In 2014, Mizuno et al. also reported the reversible protonation and deprotonation of Dawson-type silicotungstates, achieved by small apertures that act as inorganic proton receptors through intramolecular hydrogen bonds by controlling the anion charges and local electron densities of the apertures. (Figure 1.4)[26]

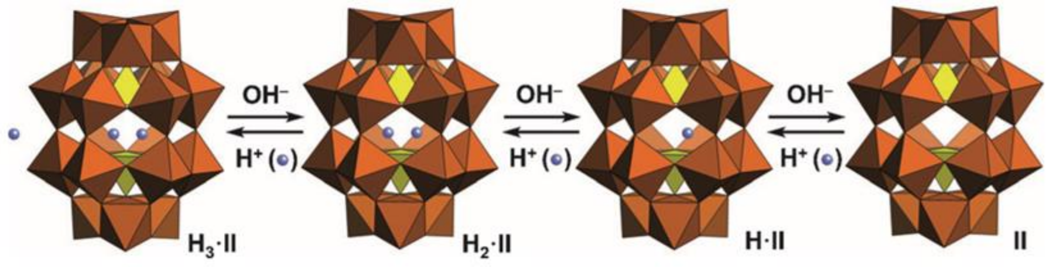

Figure 1.4. Schematic representation of reversible protonation/deprotonation of a-Dawson-type POM, II= $TBA_8[a\text{-}Si_2W_{18}O_{62}]\cdot 3H_2O$, triggered by the introduction of TBAOH and nitric acid. The atoms are represented by polyhedral and spheres: W, orange; Si, yellow; H, blue. Copyright © 2014 Wiley-VCH Verlag GmbH&Co. KGaA, Weinheim

1.3. Introduction to lanthanides

The series of 15 metallic chemical elements with atomic numbers 57-71, from lanthanum through lutetium, are named lanthanide or lanthanoid. They are called lanthanides because the elements in the series behave chemically similar to lanthanum. The informal chemical symbol Ln is used to refer to any lanthanide. These 15 elements as well as two chemically similar elements, scandium and yttrium, are known as the rare earth elements.

1.3.1. Electronic configuration and valance state

For lanthanides, their general electronic configuration is $[Xe]4f^{0-14}5d^{0-1}6s^2$. Their electronic filling does not obey the Aufbau principle simply, instead, they exert some irregularities, that is the irregular filling of 4f and 5d electrons to sustain low energy states.

Due to similar configurations in the two outermost shells, lanthanides exhibit typical metallic properties in chemical reactions. They tend to lose three electrons and exhibit a 3+ valence state. The metal reactivity gradually decreases from lanthanum to lutetium. They can react with water and release hydrogen. According to Hund's rule, electron shells are stable when empty, full, or half-full. Therefore, the configurations $4f^0$ (La^{3+}), $4f^7$ (Gd^{3+}), and $4f^{14}$ (Lu^{3+}) are stable. Ce^{3+}, Pr^{3+}, and Tb^{3+} have one or two more electrons than required for stable electronic configuration so they can be further oxidized to a 4+ state. On the contrary, Sm^{3+}, Eu^{3+}, and Yb^{3+} have one or two fewer electrons than required for a stable electronic configuration, therefore they tend to receive one or two electrons and undergo a reduction to a 2+ state.

Table 1.1. Electronic configuration of lanthanide atoms and trivalant ions

Atomic number	Element	Atomic electron configuration	Ln3+ electron configuration
57	La	$[Xe]5d^16s^2$	$[Xe]4f^0$
58	Ce	$[Xe]4f^15d^16s^2$	$[Xe]4f^1$
59	Pr	$[Xe]4f^36s^2$	$[Xe]4f^2$
60	Nd	$[Xe]4f^46s^2$	$[Xe]4f^3$
61	Pm	$[Xe]4f^56s^2$	$[Xe]4f^4$

62	Sm	$[Xe]4f^{6}6s^{2}$	$[Xe]4f^{5}$
63	Eu	$[Xe]4f^{7}6s^{2}$	$[Xe]4f^{6}$
64	Gd	$[Xe]4f^{7}5d^{1}6s^{2}$	$[Xe]4f^{7}$
65	Tb	$[Xe]4f^{9}6s^{2}$	$[Xe]4f^{8}$
66	Dy	$[Xe]4f^{10}6s^{2}$	$[Xe]4f^{9}$
67	Ho	$[Xe]4f^{11}6s^{2}$	$[Xe]4f^{10}$
68	Er	$[Xe]4f^{12}6s^{2}$	$[Xe]4f^{11}$
69	Tm	$[Xe]4f^{13}6s^{2}$	$[Xe]4f^{12}$
70	Yb	$[Xe]4f^{14}6s^{2}$	$[Xe]4f^{13}$
71	Lu	$[Xe]4f^{14}5d^{1}6s^{2}$	$[Xe]4f^{14}$

1.3.2. Lanthanide contraction

Due to the poor shielding of nuclear charge (nuclear attractive force on electrons) by 4f electrons, the 6s electrons are drawn towards the nucleus. Thus, from La to Lu, with increasing effective charges, the steadily increased nuclear attraction results in smaller atomic radii. Since the increase of effective charges among lanthanide atoms is smaller than that among lanthanide trivalent ions, the radii decrease is more dramatic for lanthanide trivalent ions, leading to the ionic radius decline from 103 pm for La^{3+} to 86.1 pm for Lu^{3+}. (Figure 1.5)

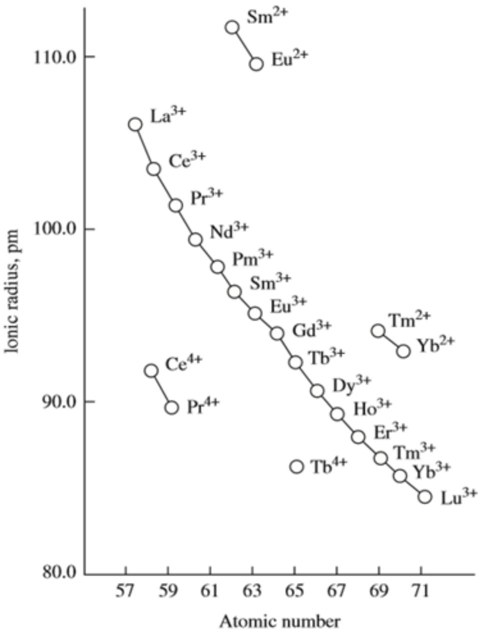

Figure 1.5. The relationship between ionic radius and atomic number of lanthanide ions.[30]

The results of lanthanide contraction may be divided into two categories: effects on the lanthanide series itself including the increase of electronegativity, the increase of covalent character (Fajuns rule), the increase of hardness, and the decrease of Lewis basicity; effects on the following or post-lanthanide elements, such as the similar properties between zirconium and hafnium.

1.3.3. Specificities of lanthanide coordination chemistry

Due to large ionic radii, lanthanide ions can accommodate large coordination numbers. Huang et al.[30] summarized 1391 coordination complexes of rare earth elements reported between 1935 and 1995, concluding all the coordination numbers are between

3 and 12, and the most common coordination number is eight (37%)(Figure1.6). Lanthanide elements have larger coordination numbers compared with transition metals with coordination numbers generally as four or six, and the variable coordination numbers are derived from the much smaller coordinating stabilization energy (about 4.18 kJ/mol) than the crystal field stabilization energy of transition metals (more than 418 kJ/mol).

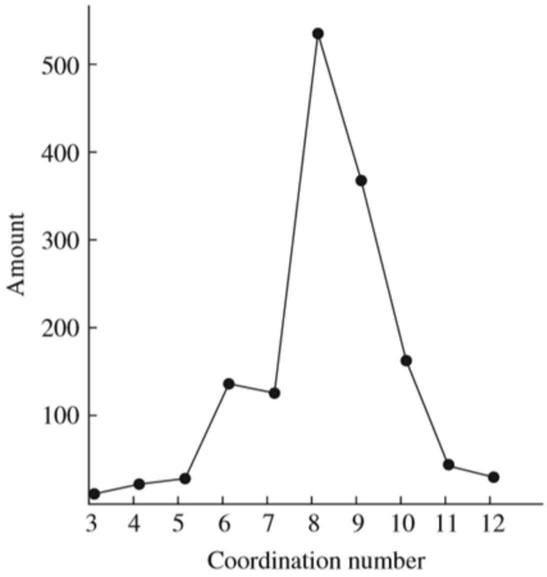

Figure 1.6. Distribution of coordination numbers among rare earth complexes (Sc, Y, La-Lu), supported by 1389 structurally characterized coordination complexes published between 1935 and 1995.[30]

The effective radii of lanthanide ions vary with different coordination numbers and different valence states: for the same ion, larger coordination numbers lead to larger effective ionic radii; for the same element with a certain coordination number, higher chemical valence leads to a smaller effective radius. Because the geometrical arrangement around the lanthanide trivalent ions highly depends on the steric properties of ligands, control of the coordination numbers can be achieved by the delicate design of ligand molecules. [31]

The coordination chemistry of lanthanide inorganic compounds is well understood. To form coordination bonds with lanthanides, the donor can be O atoms, which are the most common donors, N, S, Se, and Te atoms. A variety of compounds are reported including lanthanide hydroxides, cyanide and thiocyanate compounds, carbonate compounds, oxalate compounds, nitrate compounds, phosphate compounds, and borate compounds, etc.

1.3.4. Lanthanide polyoxometalate complexes

With oxygen-rich compositions, polyoxometalates are easily combined with highly oxyphilic lanthanide ions to form a vast number of different compounds, which display a large diversity in their structures, properties and applications in material science, catalysis, medicine. Based on the location of lanthanides within the POM complexes, the lanthanide POMs can be classified into two categories: Ln-POM clusters where lanthanides are involved in the structure of individual clusters; and extending structural Ln-POMs complexes, where discrete POM clusters act as building blocks and are connected by lanthanide linkers into one-, two-, three-dimensional structural RE-POM complexes. [30,32]

1.4. Study motivation

POMs usually act as weak nanoacid in aqueous solutions, and the acidity of POMs plays a significant role not only in their solution behaviors[17,27] but also in their broad applications as catalysts[33], biologically active materials[34], etc. Their acidity feature is sometimes related to the deprotonation behaviors of POMs. Therefore, it is reasonable to assume that studies on the deprotonation of POMs can help people understand the nature of POMs, especially the acidity feature, for further exploring POM-based materials and devices.

In this work, a series of lanthanide clusters with the formula $[K_{22}\{Nb_{12}P_4W_{24}O_{122}\}_2\{X(H_2O)_{4.5}\}_4\{Nb_4O_4(OH)_6\}] \cdot 18H_2O$, X represents lanthanide elements, are applied as model systems to study the deprotonation of these clusters, which is related to the relative strength of coordinated water molecules and further determines the acidity feature of the POM clusters. According to Xiao's work,[35] the two-stages deprotonation process is expected. The structure of the lanthanide cluster is shown in Figure 1.7.[36]

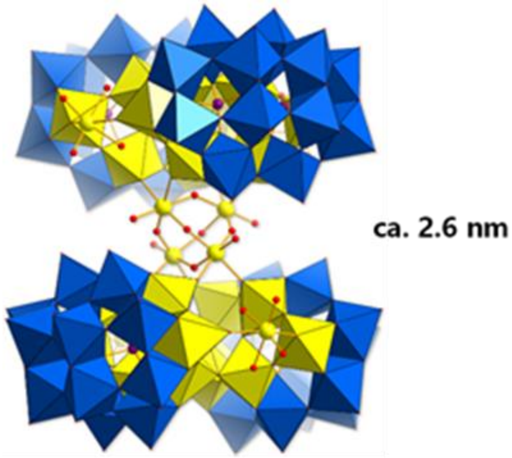

Figure 1.7. Polyhedral and ball-and-stick representation of polyanion structure. All cations and crystal water molecules are omitted for clarity. Color code: WO_6, blue polyhedra; NbO_6, yellow polyhedra; Nb, yellow balls in central portion; Ln, yellow balls linked with yellow polyhedra; P, purple balls; O, red balls.

CHAPTER II

EXPERIMENT

2.1. Sample preparation

A series of 2 mL 1ml/mL ($5.6 \cdot 10^{-5}$ mol/L) POM (Sm) and POM (Er) aqueous solutions were prepared in glovebox by dissolving crystal POMs in deionized water (boiled for exclusion of CO_2). The general chemical formula of these POMs is $[K_{22}\{Nb_{12}P_4W_{24}O_{122}\}_2\{X(H_2O)_{4.5}\}_4\{Nb_4O_4(OH)_6\}] \cdot 18H_2O$, where X represents lanthanide elements. All solutions were tightly sealed in 5 mL glass tubes. Base solutions with steadily increasing KOH equivalence (10 eq., 20 eq., …90 eq.) were added into these POM solutions, respectively. A series of 2 mL pure water with the same amount of KOH solution were prepared as blank controlled groups. The decrease of concentration of POMs was corrected during calculation. POM (Sm) and POM (Er) aqueous solutions with the same concentration and volume without addition of base were prepared for pH measurement and conductivity measurement.

To prepare KOH aqueous solution for acid-base titration, the concentration of KOH tablet was standardized by potassium hydrogen phthalate (KHP) aqueous solution and phenolphthalein, since KOH easily absorbs water and carbon dioxide.

2.2. pH Meter

The SevenExcellence^{TM} bench meter was applied for measuring pH values. All the experiments related to pH values, including solutions preparation and pH measurements, were conducted in glovebox at room temperature around 22°C. Before pH measurements, the electrode was calibrated with three buffer solutions: 0.05 mol/L $KHC_8H_4O_4$ aqueous solution with theoretical pH as 4.000 at 22°C; 0.01 mol/L $Na_2B_4O_7\cdot10H_2O$ aqueous solution with theoretical pH as 9.208 at 22°C; saturated $Ca(OH)_2$ aqueous solution with theoretical pH value as 12.553 at 22°C. These buffer solutions were chosen to cover the pH range of the sample solutions. The pH values of sample solutions prepared in section 2.1 were measured by the pH meter.

2.3. Conductivity Meter

4063 Traceable Portable Conductivity Meter was applied for conductivity measurements. Before measurements, the conductivity meter was calibrated by four standard solutions.

2.4. Isothermal Titration Calorimetry (ITC)

The isothermal titration calorimetry (ITC) measurements were conducted on a commercial TA Instruments Nano ITC system. 23.21 mM KOH aqueous solutions (250 µL) were titrated into 1 mL 0.056 mM POM solutions with deionized water in the reference cell. The background heat was subtracted by titrating 23.21 mM KOH into deionized water.

All the data were analyzed by Nano Analyze Software from the TA instrument and fitted by multiple sites model. The temperature of the cell was set at 22 °C which is consistent with the temperature when conducting acid-base titration in the glovebox.

CHAPTER III

RESULTS AND DISCUSSION

3.1. Dissociation and deprotonation of POMs in pure water

The pH values and conductivities of 1 mg/mL POM(Sm) aqueous solution, POM(Er) aqueous solution and boiled deionized water were measured, respectively. The results of measurements are shown in Table 3.1.

Table 3.1. Results of pH and conductivity measurements of POMs solutions and water

	POM(Sm)	POM(Er)	H_2O
pH	5.329	5.233	6.861
Conductivity (μS/cm)	72.4	64.4	--

Due to the slow movement of POM macroanion clusters, their contribution to conductivity is negligible, thus the conductivity of POM aqueous solution is attributed to H^+, OH^-, and K^+. The conductivity follows the equation $\kappa = \Lambda_m \cdot c$, where Λ_m is the molar conductivity and c is the molar concentration of the electrolyte solution. Therefore, the concentration of potassium ions can be calculated based on the measured pH value and conductivity. The molar conductivity values are $\Lambda_m(H^+) \approx 31.084$, $\Lambda_m(OH^-) \approx 17.594$ and $\Lambda_m(K^+) \approx 6.533$ at 20°C (unit: mS·m^2/mol) (There are no reported molar conductivity values at 22°C). Since all the free potassium ions came from the dissociation of POM clusters, the charge of each POM cluster can be approximately calculated as the concentration of K^+ divided by the concentration of POMs. According to calculation, each POM (Sm) and POM (Er) cluster dissociated 19 and 17 K^+ in pure water, thus they carried 19 and 17 negative charges, respectively. From the pH values, there is no proton released from the POM clusters when they are dissolved in pure water.

3.2. Deprotonation of POMs studied by acid-base titration

To study the deprotonation behavior of these lanthanide clusters, aqueous solutions of KOH with different equivalence were titrated into POM aqueous solution and pure water as blank controlled groups. The pH values of these solutions are shown in Table 3.2.

Table 3.2. pH values of POM and KOH aqueous solutions at different molar ratios

Molar ratio KOH:POM	KOH	POM (Sm)	KOH	POM(Er)
0	6.8	4.766	7.136	5.152
10	10.668	7.342	10.528	7.863
20	10.969	8.594	10.823	8.76
30	11.141	9.759	11.018	9.726
40	11.264	10.43	11.132	10.388
50	11.388	10.804	11.229	10.719
60	11.396	10.997	11.29	10.899
70	11.498	11.139	11.366	11.074
80	11.555	11.239	11.419	11.149
90	11.594	11.319	11.468	11.234

The significant decrease of pH values from POM/KOH aqueous solutions to corresponding KOH aqueous solutions indicated the deprotonation of POM clusters upon the trigger of additional base. The numbers of released protons from each cluster were calculated by the following equation. ($K_w \approx 0.8118 \cdot 10^{-14}$ at 22°C).

$$The\ number\ of\ released\ protons = \frac{[OH^-]_{H2O/KOH} - [OH^-]_{POM/KOH}}{[POM]}$$

The deprotonation behaviors, that is the number of released protons from POMs in different solution environments, were summarized in Table 3.3 and Figure 3.1.

Table 3.3. The number of released protons from individual cluster at different molar ratios

Molar ratio KOH:POM	10	20	30	40	50	60	70	80	90
POM (Sm)	7.1	14.7	21.8	26.8	32.1	27.6	33.8	36.7	37.6
POM (Er)	5.1	10.5	16.3	19.1	20.9	21.4	21.8	24.1	25.1

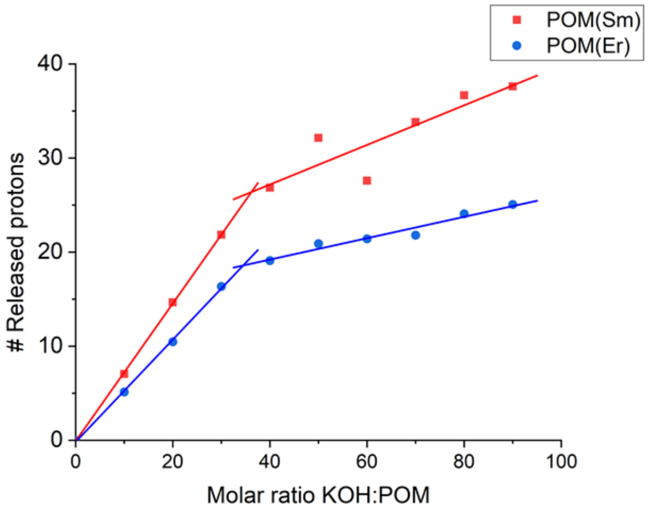

Figure 3.1. The number of released protons from individual POM cluster at different molar ratios.

The numbers of released protons are less than the equivalence of added KOH, suggesting these POMs act as weak acids in aqueous solutions. With the addition of KOH, the deprotonation process has two stages, instead of responding linearly, which is consistent with Xiao's previous observation. The intersection point of the two linear fitting lines represents the maximum number of the released protons from individual POM in the first stage. From Figure 3.1, POM (Sm) and POM (Er) clusters can release 26 and 19 protons easily in their first stage of deprotonation, and then release 11 and 6 protons more difficult in their second stage of deprotonation, respectively. In general, water molecules tend to deprotonate hydrogen ions much easier than hydroxide ions. Therefore, it is reasonable to assume here that the water ligands coordinated with lanthanide ions are easier to deprotonate than the hydroxide groups linked with niobium.

Consequently, according to the numbers of released protons, it is speculated that for POM (Sm), each cluster release 26 protons from the water ligands coordinated with samarium and the hydroxide groups linked with niobium in the first stage, then 11 protons are released from the hydroxide groups coordinated with samarium (After deprotonation in the first stage, water ligands become hydroxide groups.) in the second stage; and for POM (Er), each cluster release 19 protons from the water ligands coordinated with erbium in the first stage, and then 6 protons are released from hydroxide groups linked with niobium in the second stage. As for the difference among deprotonation behavior of POM (Sm) and POM (Er), experiments of other lanthanide POMs are expected to conduct to provide further evidence and explanation.

3.3. Deprotonation of POMs studied by ITC

To verify the deprotonation behavior, ITC measurements were conducted for binding stoichiometry, as well as the thermodynamic parameters during the interaction. The results of ITC measurements and the fitting are shown in Figure 3.2 and Figure 3.3.

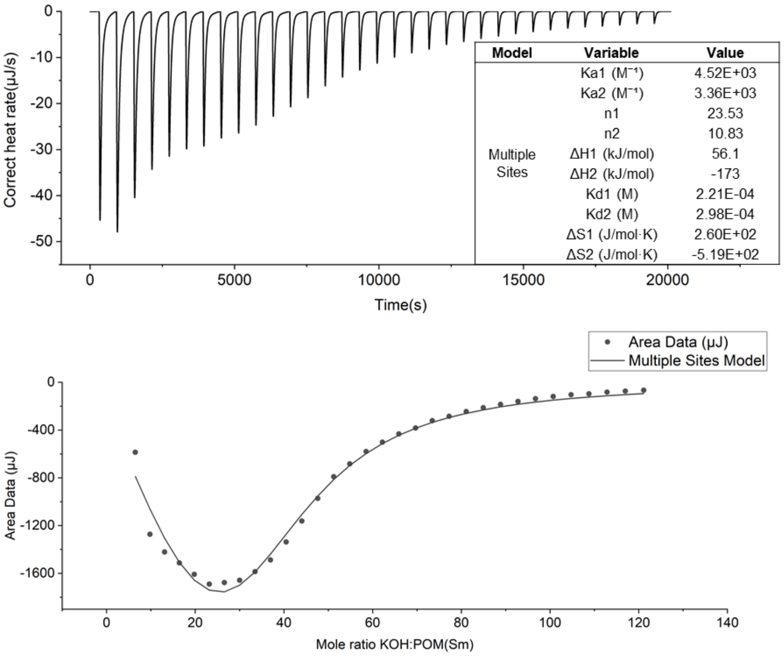

Model	Variable	Value
Multiple Sites	Ka1 (M^{-1})	4.52E+03
	Ka2 (M^{-1})	3.36E+03
	n1	23.53
	n2	10.83
	ΔH1 (kJ/mol)	56.1
	ΔH2 (kJ/mol)	-173
	Kd1 (M)	2.21E-04
	Kd2 (M)	2.98E-04
	ΔS1 (J/mol·K)	2.60E+02
	ΔS2 (J/mol·K)	-5.19E+02

Figure 3.2. ITC thermograms and isotherms by titrating 23.21 mM KOH aqueous solution into 0.056 mM POM (Sm) aqueous solutions at 22 °C. Fitting model: Multiple sites model.

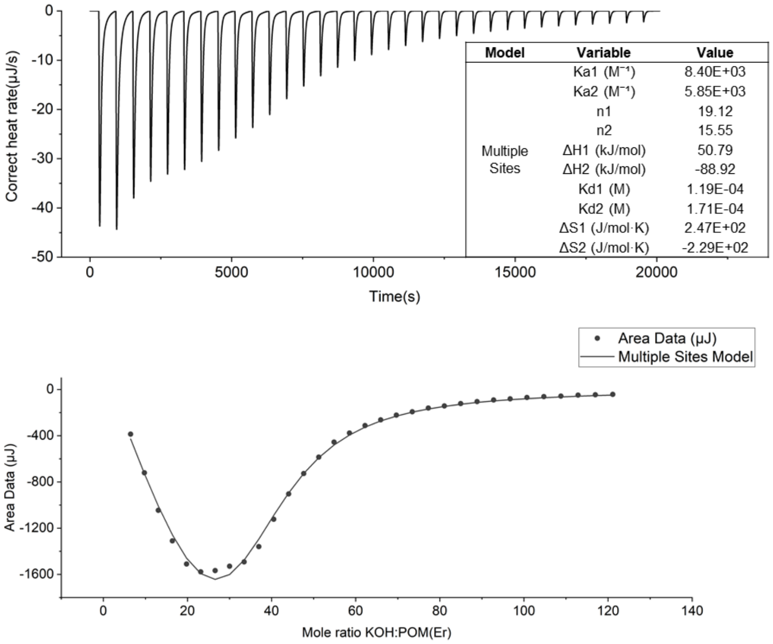

Model	Variable	Value
Multiple Sites	Ka1 (M^{-1})	8.40E+03
	Ka2 (M^{-1})	5.85E+03
	n1	19.12
	n2	15.55
	ΔH1 (kJ/mol)	50.79
	ΔH2 (kJ/mol)	-88.92
	Kd1 (M)	1.19E-04
	Kd2 (M)	1.71E-04
	ΔS1 (J/mol·K)	2.47E+02
	ΔS2 (J/mol·K)	-2.29E+02

Figure 3.3. ITC thermograms and isotherms by titrating 23.21 mM KOH aqueous solution into 0.056 mM POM (Er) aqueous solutions at 22 °C. Fitting model: Multiple sites model.

The number of binding sites (n) here represents the number of protons that reacted with the additional KOH. As the molar ratio between KOH and POM is large enough, there is no more detectable interaction when titration reaching the end, because the heat change is slight and negligible at that time. From the fitting results, the Ka1 value is higher than the Ka2 value for both POM (Sm) and POM (Er), which means that the first interaction is more favorable than the second interaction. The first interaction is attributed to acid-base reaction, that is the deprotonation, and the second interaction is attributed to the association of potassium ions and the POM macroanion clusters. The number of binding sites in the first interaction is consistent with the number of released protons in the first stage in the pH titration experiments. ITC cannot measure the number of released protons in the second stage obtained in the pH titration experiments due to the low binding strength in the second stage.

CHAPTER IV

CONCLUSION

In summary, the deprotonation of POM (Sm) and POM (Er) upon the trigger of the additional base in aqueous solutions was explored. There are no protons released from these two lanthanide clusters in pure water, and their two-stages deprotonation behaviors vary with different lanthanides. The difference among the deprotonation of the two lanthanide clusters might derive from different deprotonation sites and different coordination strengths caused by lanthanide contraction. To further verify and explain the effect of different lanthanides on the deprotonation, experiments of other POMs, such as POM (Lu), are needed.

BIBLIOGRAPHY

1. Liu, T. Hydrophilic macroionic solutions: What happens when soluble ions reach the size of nanometer scale? *Langmuir* **26**, 9202–9213 (2010).

2. Hückel, E. & Debye, P. The theory of electrolytes: I. lowering of freezing point and related phenomena. *Phys. Z* **24**, 1 (1923).

3. Verwey, E. J. W. Theory of the stability of lyophobic colloids. *J. Phys. Chem.* **51**, 631–636 (1947).

4. Yin, P. Polyoxometalates Macroions : From Self- Recognition to Functional Materials. (2013).

5. Sun, X. *et al.* Role of Protein Charge Density on Hepatitis B Virus Capsid Formation. *ACS omega* **3**, 4384–4391 (2018).

6. Eghtesadi, S. A., Haso, F., Kashfipour, M. A., Lillard, R. S. & Liu, T. Supramolecular Assembly of Poly(propyleneimine) Dendrimers Driven by Simple Monovalent Counterions. *Chem. - A Eur. J.* **21**, 18623–18630 (2015).

7. Li, H. *et al.* Adjusting emission wavelength by tuning the intermolecular distance in charge-regulated supramolecular assemblies. *J. Phys. Chem. C* **123**, 23280–23286 (2019).

8. Borrás-Almenar, J. J., Coronado, E., Müller, A. & Pope, M. *Polyoxometalate molecular science*. vol. 98 (Springer Science & Business Media, 2003).

9. Long, D.-L., Burkholder, E. & Cronin, L. Polyoxometalate clusters, nanostructures and materials: From self assembly to designer materials and devices. *Chem. Soc. Rev.* **36**, 105–121 (2007).

10. Gouzerh, P. & Che, M. From Scheele and Berzelius to Müller: Polyoxometalates (POMs) revisited and the missing link between the bottom up and top down approaches. *Actual. Chim.* 9–22 (2006).

11. Keggin, J. F. The structure and formula of 12-phosphotungstic acid. *Proc. R. Soc. London. Ser. A, Contain. Pap. a Math. Phys. Character* **144**, 75–100 (1934).

12. Hasenknopf, B. Polyoxometalates: introduction to a class of inorganic compounds and their biomedical applications. *Front. Biosci* **10**, (2005).

13. Hill, C. L. Introduction: PolyoxometalatesMulticomponent Molecular Vehicles To Probe Fundamental Issues and Practical Problems. *Chem. Rev.* **98**, 1 (1998).

14. Liu, T., Diemann, E., Li, H., Dress, A. W. M. & Müller, A. Self-assembly in aqueous solution of wheel-shaped Mo154 oxide clusters into vesicles. *Nature* **426**, 59–62 (2003).

15. Pigga, J. M., Kistler, M. L., Shew, C., Antonio, M. R. & Liu, T. Counterion Distribution around Hydrophilic Molecular Macroanions: The Source of the Attractive Force in Self-Assembly. *Angew. Chemie Int. Ed.* **48**, 6538–6542 (2009).

16. Yin, P., Li, D. & Liu, T. Solution behaviors and self-assembly of polyoxometalates as models of macroions and amphiphilic polyoxometalate–organic hybrids as novel surfactants. *Chem. Soc. Rev.* **41**, 7368–7383 (2012).

17. Liu, T. *et al.* Deprotonations and Charges of Well-Defined {Mo72Fe30} Nanoacids Simply Stepwise Tuned by pH Allow Control/Variation of Related Self-Assembly Processes. *J. Am. Chem. Soc.* **128**, 15914–15920 (2006).

18. Kistler, M. L., Liu, T., Gouzerh, P., Todea, A. M. & Müller, A. Molybdenum-oxide based unique polyprotic nanoacids showing different deprotonations and related assembly processes in solution. *J. Chem. Soc. Dalt. Trans.* 5094–5100 (2009) doi:10.1039/b901505a.

19. Constable, E. *Comprehensive coordination chemistry II: from biology to nanotechnology*. (Newnes, 2003).

20. Ruhlmann, L., Nadjo, L., Canny, J., Contant, R. & Thouvenot, R. Di-and Tetranuclear Dawson-Derived Sandwich Complexes: Synthesis, Spectroscopic Characterization, and Electrochemical Behavior. *Eur. J. Inorg. Chem.* **2002**, 975–986 (2002).

21. Musaev, D. G., Morokuma, K., Geletii, Y. V & Hill, C. L. Computational modeling of di-transition-metal-substituted γ-Keggin polyoxometalate anions. Structural refinement of the protonated divacant lacunary silicodecatungstate. *Inorg. Chem.* **43**, 7702–7708 (2004).

22. Prabhakar, R., Morokuma, K., Hill, C. L. & Musaev, D. G. Insights into the mechanism of selective olefin epoxidation catalyzed by [γ-(SiO4) W10O32H4] 4-. A computational study. *Inorg. Chem.* **45**, 5703–5709 (2006).

23. Liu, T. *et al.* Deprotonations and charges of well-defined {Mo72Fe30} nanoacids simply stepwise tuned by pH allow control/variation of related self-assembly processes. *J. Am. Chem. Soc.* **128**, 15914–15920 (2006).

24. Sartorel, A., Carraro, M., Bagno, A., Scorrano, G. & Bonchio, M. Asymmetric Tetraprotonation of γ-[(SiO4) W10O32] 8− Triggers a Catalytic Epoxidation Reaction: Perspectives in the Assignment of the Active Catalyst. *Angew. Chemie Int. Ed.* **46**, 3255–3258 (2007).

25. Kistler, M. L., Liu, T., Gouzerh, P., Todea, A. M. & Müller, A. Molybdenum-oxide based unique polyprotic nanoacids showing different deprotonations and related assembly processes in solution. *Dalt. Trans.* 5094–5100 (2009).

26. Minato, T., Suzuki, K., Kamata, K. & Mizuno, N. Synthesis of a -Dawson-Type Silicotungstate [a -Si 2 W 18 O 62] 8 À and Protonation and Deprotonation Inside the Aperture through Intramolecular Hydrogen Bonds. 5946–5952 (2014) doi:10.1002/chem.201400390.

27. Zhang, D. *et al.* A large molecular cluster with high proton release capacity. *Chem. Commun.* **56**, 12849–12852 (2020).

28. Cotton, F. A., Wilkinson, G., Murillo, C. A., Bochmann, M. & Grimes, R. *Advanced inorganic chemistry*. vol. 6 (Wiley New York, 1988).

29. Sartorel, A., Carraro, M., Bagno, A., Scorrano, G. & Bonchio, M. H2O2 activation by heteropolyacids with defect structures: the case of γ-[(XO4) W10O32] n−(X= Si, Ge, n= 8; X= P, n= 7). *J. Phys. Org. Chem.* **21**, 596–602 (2008).

30. Chunhui Huang(Peking University). *RARE EARTH COORDINATION COORDINATION CHEMISTRY FUNDAMENTALS AND APPLICATIONS*. (2010).

31. Bünzli, J. C. G. Review: Lanthanide coordination chemistry: From old concepts to coordination polymers. *J. Coord. Chem.* **67**, 3706–3733 (2014).

32. Dolbecq, A., Dumas, E., Mayer, R. & Mialane, P. Hybrid Organic - Inorganic Polyoxometalate Compounds : From Structural Diversity to Applications. 6009–6048 (2010).

33. Sun, M. *et al.* Significant effect of acidity on catalytic behaviors of Cs-substituted polyoxometalates for oxidative dehydrogenation of propane. *Appl. Catal. A Gen.* **349**, 212–221 (2008).

34. Shi, Y. *et al.* An acidity-responsive polyoxometalate with inflammatory retention for NIR-II photothermal-enhanced chemodynamic antibacterial therapy. *Biomater. Sci.* **8**, 6093–6099 (2020).

35. Kexing Xiao(University of Akron）. DEPROTONATION PROPERTY OF POLYOXOMETALATES WITH DIFFERENT LACUNARY METAL IONS. (2019).

36. Zhang, D. *et al.* A new Nb28 cluster based on tungstophosphate,[{Nb4O6 (OH) 4}{Nb6P2W12O61} 4] 36–. *Inorg. Chem. POM Proj. - pH Meas. Lit. search/Hydrolytic Synth. Struct. Charact. of.pdf* **53**, 9917–9922 (2014).